

# Analysis of Earthquake Response of an Asphalt Concrete Core Embankment Dam

Mohammad Hassan Baziar<sup>1,\*</sup>, Shirin Salemi<sup>2</sup>, Tahereh Heidari<sup>3</sup>

\*Centre of Excellence for Fundamental Studies in Structural Engineering, Iran University of Science and Technology

<sup>1</sup>Professor, e-mail: baziar@iust.ac.ir,

<sup>2</sup>Ph.D., e-mail: salemi@iust.ac.ir,

<sup>3</sup>Senior Engineer, e-mail: t.heidari@civileng.iust.ac.ir,  
College of Civil Engineering, Iran University of Science & Technology (IUST),  
Narmak, Tehran, 16844, Iran,

**Abstract:** Seismic behavior of a rockfill dam with asphalt-concrete core has been studied utilizing numerical models with material parameters determined by laboratory tests. The case study selected for these analyses, is the Meyjaran asphalt core dam, recently constructed in Northern Iran, with 60 m height and 180 m crest length. The numerical analyses have been performed using a non-linear three dimensional finite difference software and various hazard levels of earthquakes. This study shows that due to the elasto-plastic characteristics of the asphalt concrete, rockfill dams with asphalt concrete core behave satisfactorily during earthquake loading. The induced shear strains in the asphalt core, for the case presented in this research, are less than 1% during an earthquake with  $a_{max}=0.25g$  and the asphalt core remains watertight. Due to large shear deformations caused by a more severe earthquake with  $a_{max}=0.60g$ , some cracking may occur towards the top of the core (down to 5-6 m), and the core permeability may increase in the top part, but the dam is safe.

**Keywords:** Asphalt concrete core, Dynamic analyses, Laboratory tests, Three dimensional numerical models.

## 1. Introduction

In recent years, construction of earthfill and rockfill dams with asphalt concrete core has attracted the attention of many dam designers all over the world. Construction of this type of dam in regions with cold and rainy weather, or in regions with shortage of natural earth core material, is very advantageous.

Monitoring of existing asphalt core dams have indicated their good behavior during operation, which is mainly related to the visco-elastic plastic properties of asphalt concrete [1], [2]. However, the behavior of thin asphalt cores under earthquake shaking needs further investigation. Particularly in recent years, construction of this type of dam in the seismic areas of the world such as

Japan, China and Iran has caused researchers to focus on the dynamic behavior of asphalt cores [3].

In the last decade, improvements in the different numerical methods have resulted in widespread use of these methods to study dynamic behavior of all types of earth dams [4].

Hoeg [5], and later Gurdil [6] and Ghanooni and Roosta [7] presented results of two dimensional dynamic analyses of asphalt core dams. They showed that relatively large shear strains may develop in the top of the asphalt core due to dam crest amplification of the ground motion, but concluded that the dams investigated would behave safely.

2-D response analyses of Meyjaran asphalt core dam in northern Iran, using the finite

element method and an elasto-plastic model, were carried out by the authors [8]. The results showed that the induced shear strains in the asphalt core were small enough to keep it watertight. Similar results have been obtained from three-dimensional dynamic analysis of the Alborz dam with asphalt core [9].

Many researchers have investigated the stress-strain behavior of asphalt concrete used for road pavements and the effects of dynamic traffic loading using laboratory tests. However, there are only a few papers that provide information on the behavior of asphalt concrete used as a watertight element for dams when subjected to simulated earthquake loading [3]. The first experimental research performed on the earthquake resistance of asphalt concrete core materials was conducted by Breth and Schwab [10] in Germany. They performed special cyclic triaxial tests on the asphalt concrete samples and concluded that the asphalt material under the specified cyclic stresses, behaved like an elastic body. Since then, there is no any report of laboratory tests to simulate seismic loading on asphalt core material until recently when the construction of such dams in seismic regions has renewed the interest in this issue [3].

Wang [11] recently reported a series of cyclic loading tests on triaxial specimens of asphalt concrete and concluded that there was no sign of cracking or deterioration of the asphalt concrete. Nakumara et al. [12] carried out laboratory tests to compare the engineering properties of asphalt concrete used in dam facing with Superflex-phalt (asphalt concrete with a special admixture to increase the flexibility and tension strain level prior to development of cracks).

In the present study, the response of the

Meyjaran rockfill dam, due to its location in a narrow valley, has been investigated using a three-dimensional finite difference method (FLAC 3D).

To determine the geotechnical properties of asphalt concrete for use in the numerical models and to investigate the stress-strain behavior of asphalt concrete under static and dynamic loading, laboratory tests including static and cyclic triaxial tests and wave velocity measurements have been carried out. Also, in order to investigate the effect of large shear strains on the permeability of the asphalt core material, permeability tests have been performed on the deformed samples of asphalt concrete obtained from the triaxial specimens subjected to previous shear stresses.

## **2. Location and Seismo-Tectonic Features of the Meyjaran Dam Site**

Meyjaran dam is located 20 km south-east of Ramsar City in northern Iran. It has been constructed on the Nesa River in order to supply irrigation and drinking water. It is 60 m high and has 180 m crest length. The vertical asphalt concrete core has 1-meter width and has upstream and downstream filter and transition zones. Figure 1 shows the maximum cross section of the dam. The dam is placed in a V-shaped and fairly symmetric valley underlain by a conglomerate foundation. This conglomerate is classified, based on RMR classification, as fair to good rock.

Meyjaran dam site is located in Alborz seismic zone where active periods have been observed. One of the most important earthquakes that occurred in this area is the June 1990 Manjil earthquake, with  $M_b=7.3$  and  $M_s=7.7$ . The epicenter of this earthquake

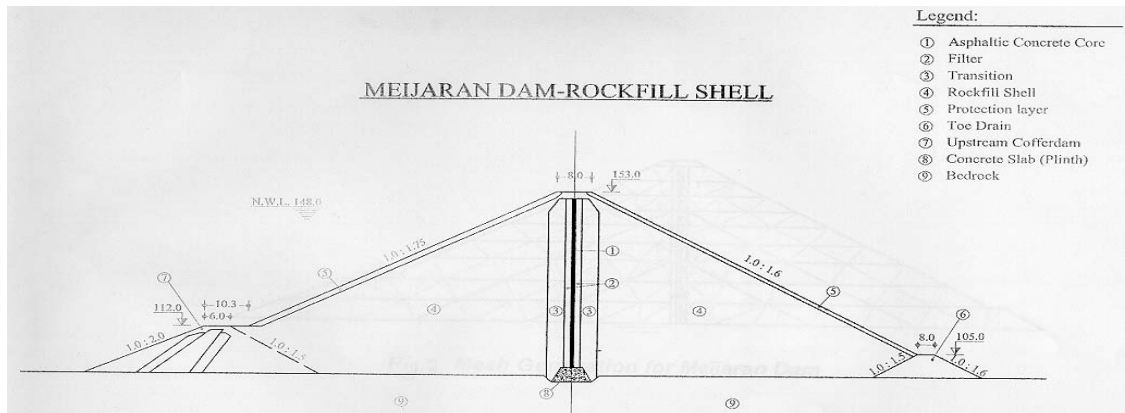


Figure 1: The typical cross section of Meyjaran dam

was about 160-km west of the Meyjaran dam site.

### 3. Laboratory Tests to Determine Geotechnical Parameters

In order to investigate the stress-strain behavior of asphalt concrete under static and dynamic loading and also to study the effect of induced strain on the permeability of this material, laboratory tests including static and cyclic triaxial tests, and permeability tests have been carried out. To determine the dynamic parameters of asphalt concrete at very low strain levels, the velocities of P- and S-waves were also measured.

#### 3-1 Specimen Preparation

The laboratory triaxial specimens were prepared in a mould with diameter of 70mm and a height of 140mm. The dry aggregates, in accordance with the weight proportions shown in Table 1, were preheated at 160°C. This is the same material as used in the asphalt core of Meyjaran dam (after removing the grains bigger than 18mm). The B60 bitumen was preheated at 150°C. The hot aggregates and bitumen were placed in a

heated mixer. At a temperature between 140° to 150°C, the mixture was placed and compacted in a preheated cylindrical mould with an inside diameter of 70mm. After compaction and cooling, the specimen was taken out of the mould.

The compaction method used to prepare the specimens was similar to the Marshall Compaction procedure described by Weibiao and Hoeg [13]. The asphalt concrete mix was compacted in three consecutive layers, each originally with approximately 60mm thickness. Each layer was compacted by 30 blows (one blow per second) of a hammer with a flat circular tamping surface of 6.7mm diameter. The hammer has 4.5kg weight and the height of its drop is 450mm.

#### 3-2 Static Triaxial Tests

All the static triaxial tests were strain-controlled compression tests with axial stress increasing and lateral confining stress held constant. The confining stress was varied from 0.1 to 0.5 MPa. The strain rate was 0.1% per minute. The magnitude of axial stress, axial strains and volumetric strain were recorded throughout the tests. The testing temperature was 19 °C.

Table 1: Geotechnical parameters of Meyjaran dam

Type of Material	K*	N*	k <sub>b</sub> **	M**	C kg/cm <sup>2</sup>	Φ	γ <sub>wet</sub> gr/cm <sup>3</sup>
Asphalt core	280 to 355	0.36 to 0.62	759 to 1710	0.32 to 0.68	3	25	2.4
filter	864	0.64	977	0.7	0	40	2.10
gravel	700	0.6	500	0.6	0	45	2.05

\* “k” and “n” are the model parameters (constants) relating to the initial modulus, E<sub>i</sub>, in a hyperbolic model. Where  $E_i = k P_a (\sigma_3 / P_a)^n$  and P<sub>a</sub> is the atmospheric pressure .

\*\* “k<sub>b</sub>” and “m” are dimensionless parameters (constants) relating to bulk modulus, B, in a hyperbolic model. Where  $B = k_b P_a (\sigma_3 / P_a)^m$ .

Table 2: Summary of results of dynamic Analysis of the asphalt core dam

Description	E.Q. Loading		
	DBL. E.Q. a <sub>max</sub> =0.25g	MDL. E.Q. a <sub>max</sub> =0.5g	MCL EQ. a <sub>max</sub> =0.6g
Max. Acceleration at dam Crest. (g)	0.73	0.89	1.6
Max. Horizontal disp. at dam crest (cm)	6.3	18.7	30
Max. vertical disp. at Core (cm)	2	10	18
Max. Core shear strain (%)	< 1	6	14

The test results summarized in Table 2, show very ductile plastic behavior after the strength level has been reached. Brittle failure was not observed in any of those tests. Young modulus (secant modulus at 1 percent axial strain) is between 90 to 150 MPa for the various specimens with 6.0% bitumen content. The average secant shear modulus,

G<sub>s</sub> at the same axial strain is obtained to be around 45 MPa. Figure 2 shows the stress-strain curve in one series of these tests with confining stress equal to 0.3 MPa .

### 3-3 Cyclic Triaxial Tests

Cyclic triaxial tests were carried out on

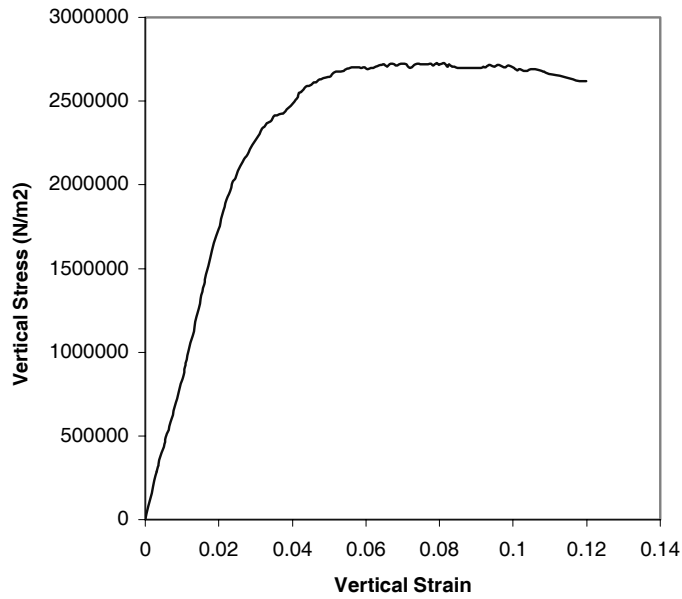


Fig. 2: Stress- strain curve from the static triaxial test (TS-3)

Table 3: Information of asphalt concrete mix used in this study

Diameter of particle (mm)	percentage of particles passing	bitumen content (%)
18	100	5 to 7
12.7	82	
9.51	70	
4.76	51	
2	31	
1.19	24	
0.63	14	
0.33	6	
0.15	2	
0.075	1	

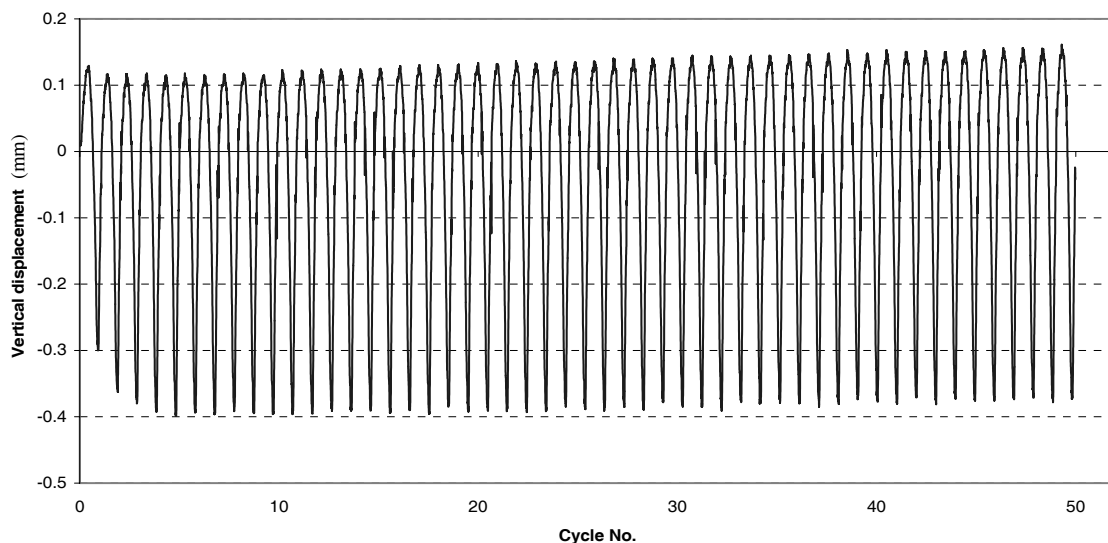


Fig.3: Variation of vertical displacement during cyclic loading

samples prepared with the specifications mentioned above. These tests were loaded under isotropic consolidation with different confining stress and also under an-isotropic consolidation with  $\sigma_3/\sigma_1=0.25$  to simulate in-situ conditions. These states of static stresses were superimposed by a cyclic shear stress of 0.1 to 0.2 MPa with a frequency of 2 Hertz. This range of cyclic loads corresponds approximately to the load of earthquakes with Richter magnitude 6.0 to 6.8, acting on Meyjaran rockfill dam with asphalt concrete core. Table 3 summarizes the specifications of these tests.

Figure 3, as an example, shows the variation of axial displacement during cyclic loading in one test ( $T_5S_3C_4$ ). As it is seen, the cyclic strain amplitudes under cyclic stress remain almost constant and the residual strains are negligible. In other words, the induced deformations at this level of strain are virtually elastic. This is similar to the test results reported by Wang [11].

The 200 load cycles imposed did not change

the structure and strength properties of the samples. The induced deformations were small and there was not any sign of fissuring or cracking in the specimens. The maximum shear strain recorded in the samples with 6.0% of bitumen was 0.4%.

Figure 4 shows the shear modulus vs. shear strain ( $G-\gamma$ ) relationship of the asphalt concrete in one cycle during increasing load. It can be seen that the dynamic shear modulus,  $G$ , of the asphalt mixture is strongly dependent on the shear strain. At very small strains, the  $G$  values are very high but decrease rapidly with increasing shear strain. At  $\gamma=0.003\%$ , the  $G$  value is around 1600 MPa, but decreases to about 100 MPa (less than one tenth of its initial value) at  $\gamma=0.1\%$ . Similar results have been obtained by Nakamura [12], but with higher values of shear modulus.

### 3-4- Measurement of P-wave and S-wave Velocities by the Pulse Method

P-wave and S-wave velocities were

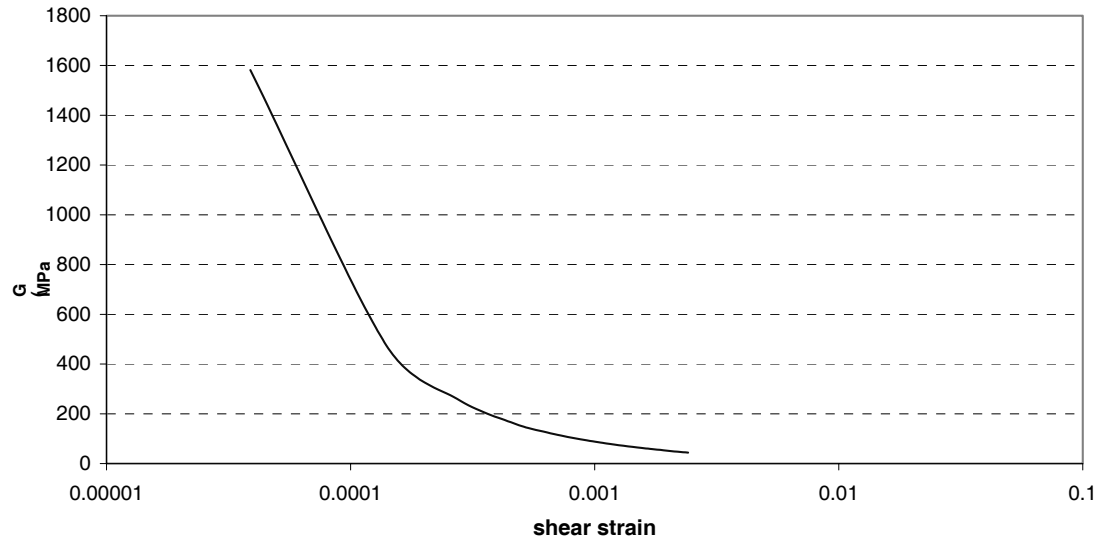


Fig.4:  $G-\gamma$  relationship of the asphalt material

Table 4: The static triaxial test results

Test No.	Confining stress, $\sigma_3$ (MPa)	Axial stress at failure, $\sigma_1$ (MPa)	$\sigma_1/\sigma_3$ at failure	Axial strain at failure %	Young's modulus (at 1% strain) (MPa)
TS-1	0.1	1.2	12	16	90
TS-2	0.2	1.9	9.5	16	95
TS-3	0.3	2.7	9	12	100
TS-4	0.4	3.2	8	14	140
TS-5	0.5	3.8	7.6	14	150

Table 5: Specification of cyclic triaxial tests

Test No.	bitumen content (%)	Loading Condition	Confine Pressure ( $\sigma_3$ ) (MPa)	Static deviator Stress ( $\sigma_1 - \sigma_3$ ) (MPa)	$\sigma_3/\sigma_1$	Cyclic Axial Stress (MPa)
T <sub>1</sub> S <sub>1</sub> C <sub>25</sub>	6.0	Isotropic	0.25	-	1	0.24
T <sub>2</sub> S <sub>2</sub> C <sub>5</sub>	6.0	An-isotropic	0.05	0.15	0.25	0.2
T <sub>3</sub> S <sub>5</sub> C <sub>25</sub>	5.0	Isotropic	0.25	-	1	0.24
T <sub>4</sub> S <sub>7</sub> C <sub>25</sub>	7.0	Isotropic	0.25	-	1	0.24
T <sub>5</sub> S <sub>3</sub> C <sub>4</sub>	6.0	Isotropic	0.4	-	1	0.4
T <sub>6</sub> S <sub>8</sub> C <sub>4</sub>	7.0	Isotropic	0.4	-	1	0.4
T <sub>7</sub> S <sub>9</sub> C <sub>25</sub>	6.0	An-isotropic	0.05	0.15	0.25	0.2
T <sub>8</sub> S <sub>10</sub> C <sub>4</sub>	7.0	Isotropic	0.4	-	1	0.4
T <sub>9</sub> S <sub>4</sub> C <sub>4</sub>	6.0	Isotropic	0.4	-	1	0.4

measured in asphalt specimens with 5cm and 14cm length. In these tests, a sensor is connected to each end of the sample and an electrical pulse is transmitted to the top sensor and the input pulse is received at the other end. The time interval ( $\Delta t$ ) between sending and receiving of signals is recorded and monitored by oscilloscope. The wave velocity is obtained by dividing the length of sample with the time interval. The results of the tests are shown in the Table 4 which indicates a high value of 3800-4100 MPa for the shear modulus of the asphalt concrete, compatible with the results of the cyclic triaxial tests at very low shear strains.

### 3-5 Permeability Test

Permeability tests were performed on horizontal disc samples which were cut from the monotonically loaded triaxial specimens after applying different levels of axial strains (3%, 6%, 10%, and 14%). The asphalt discs with 4cm thickness were put in the steel mould in the triaxial cell under a water

pressure of 50 kPa. Bitumen was used for filling the space between mould and sample to ensure that water could flow only through the asphalt disc. The water flowing through the asphalt sample was measured during 48 hours.

The results show that for the specimens with the imposed axial strains of 3% and 6% which corresponds to shear strains of 4.4% and 8.7%, the permeability of the asphalt concrete was not increased significantly as the asphalt still remained virtually watertight. However, the permeability of the specimens under axial strains of 10% were increased and it reached around 10-5cm/s at an axial strain of 14% (Table 5).

### 3-6- Selection of Shear Modulus for use in dynamic analysis

One of the important parameters for dynamic analysis is the selection of shear modulus. To determine the shear modulus of various granular soils and rockfill at very low levels



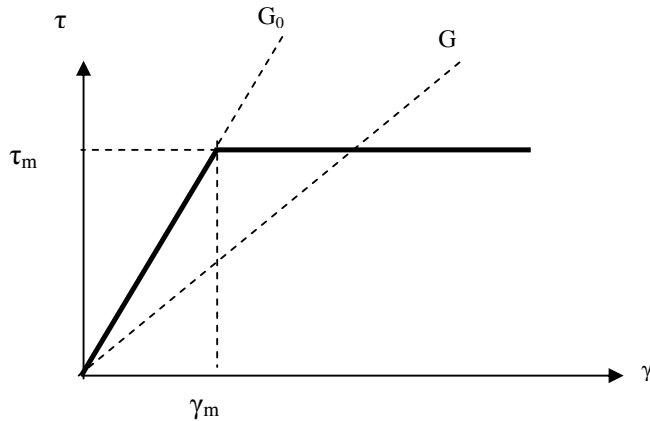


Fig. 5: Shear Modulus Reduction with Strain in Elastic-plastic Mohr-Coloumb Model

of strain, ( $G_{max}$  or  $G_0$ ), a number of empirical formula based on laboratory tests (resonant column and cyclic triaxial tests) have been proposed by several researchers [14]. For coarse-grained soil and for a sufficiently small shear strain of  $\gamma=10^{-5}$ , the shear modulus,  $G_0$ , is given by Kokusho [15].

For filter material,  $G_0$  was calculated using equation:

$$G_0 = 8400 \frac{(2.17 - e)^2}{1 + e} (\sigma_0)^{0.60}$$

For the shell material of the dam,  $G_0$  was calculated by the equation:

$$G_0 = 13000 \frac{(2.17 - e)^2}{1 + e} (\sigma_0)^{0.55}$$

where  $\sigma_0$  is the mean effective stress.  $G$  and  $\sigma_0$  are both in kPa and “ $e$ ” is the void ratio of the material.

From the cyclic triaxial tests on the asphalt concrete samples,  $G_{max}$  was selected to be 1000 MPa, for the small shear strain of  $\gamma=5 \times 10^{-5}$ . However, sensitivity analyses showed that the change of maximum shear modulus in the range of 800-1800 MPa did not have significant effects on the dynamic

response of the dam.

In a fully non-linear method of dynamic analyses, contrary to the equivalent-linear method, the dependence of shear modulus and damping on strain level are automatically modeled. The elastic-plastic model of Mohr-Coulomb can produce curves of apparent damping and modulus versus cyclic strain over limited strain ranges [16]. In Figure 5, an elastic-plastic model with a constant shear modulus,  $G_0$ , and a constant yield stress,  $\tau_m$ , is shown. If this model is subjected to a cyclic shear strain of amplitude  $\tilde{\gamma}$  below the yield strain, the secant shear modulus,  $G$ , is simply equal to  $G_0$ . For cyclic excitation that involves yielding, the secant modulus is:

$$G = \tau_m / \gamma \quad (1)$$

where  $\tau_m = \tau_0 \tan \varphi$  is the material strength and is expressed by the Mohr-Coulomb failure criterion:

$$\tau_m = \tau_0 \tan \varphi \quad (2)$$

The maximum stored energy,  $W$ , during the cycle (assuming  $G$  represents an elastic modulus) is:

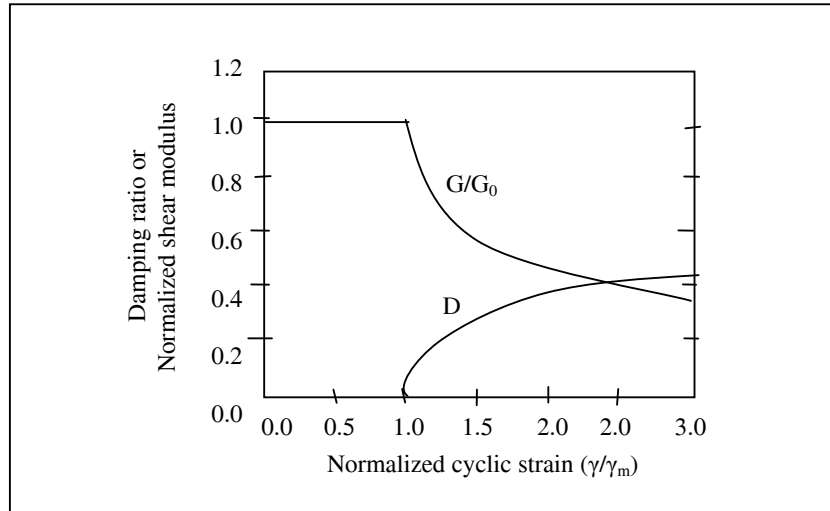


Fig. 6: normalized modulus,  $(G/G_0)$  and damping,  $D$ , versus normalized cyclic strain, (Itasca,1997)

$$W = \tau_m \gamma / 2 \quad (3)$$

and the dissipated energy (corresponding to the area of the loop) is:

$$\Delta W = 4 \tau_m (\gamma - \gamma_m) \quad (4)$$

where  $\gamma_m = \tau_m / G_0$ . Hence,

$$\Delta W / W = 8 (\gamma - \gamma_m) / \gamma \quad (5)$$

Denoting the damping ratio by  $D$  and noting that  $4\pi D \sim \Delta W / W$ , for small  $D$  [17]:

$$D = 2 (\gamma - \gamma_m) / \pi \gamma \quad (6)$$

Figure 6 shows the normalized modulus,  $(G/G_0)$ , from Eq.(1) and damping,  $D$ , from Eq. (6) versus normalized cyclic shear strain  $(\gamma / \gamma_m)$ .

#### 4 Numerical Analyses

The numerical modeling for the static and dynamic analyses has been performed using the FLAC3D program [16], which is based

on the finite difference method. The dam with its foundation (down to 60m) was modeled three-dimensionally by generating different types of elements including bricks, wedges, pyramids and tetrahedrons. For accurate representation of wave transmission in the model, the element sizes have been selected small enough to satisfy the following criteria expressed by Kuhlemeyer & Lysmer [18]:

$$\Delta l \leq \frac{\lambda}{10} \quad (7)$$

where  $\lambda$  is the wave length associated with the highest frequency component that contains appreciable energy, and  $l$  is the length of element. The maximum element size in the direction of dam height is 2.75m and in other directions it varies up to 5m. Therefore, frequencies up to 20 Hz may be transmitted through the asphalt core. The boundaries have been considered as viscous in the dynamic analyses. Figure 7 shows the geometry of the model and its grid.

The dam embankment construction was modeled with 20 layers of compacted fill. The hyperbolic stress-strain model proposed

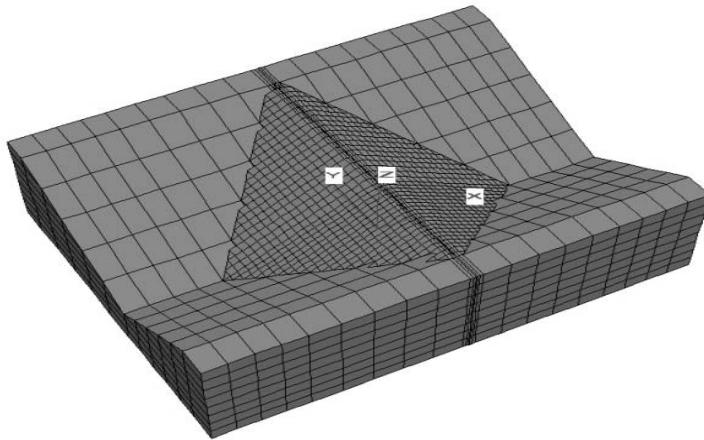


Figure 7: Three-Dimensional model of the dam and its foundation

Table 6: Information regarding P- and S-waves Velocities using Pulse Method

Length of Sample (cm)	Time recorded for receiving P-wave ( $\mu$ s)	P-waves average velocity (m/s)	Time recorded for receiving S-wave ( $\mu$ s)	S-waves average velocity (m/s)	Shear modulus $G=V_s^2\rho$ (MPa)
14	55.8	2509	110.6	1266	3846
5	17.93	2788	38.06	1314	4143

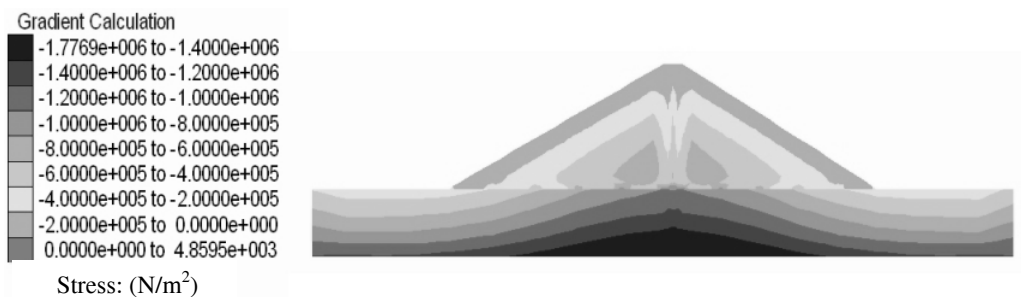


Figure 8: Vertical stress contours on dam cross-section (static analyses)

by Duncan and Chang [19] was used for the static stress calculations.

Dynamic response analyses were carried out for the end of construction stage, under different earthquakes, using the Mohr-Coulumb model for material behavior. Previous research [8] indicated that deformations in the asphalt concrete core, at the end of construction stage are more critical than for the stage with full reservoir and steady state seepage. Therefore the results of dynamic analysis for an empty reservoir are presented here.

The geotechnical parameters for the dam body were discussed in sections 3-2 and 3-6 and are presented in Table 6.

#### 4-1 Static Analyses

For the end-of-construction stage, the contours of vertical stress for the cross section at the middle of the dam axis are shown in Figure 8. As is seen, the vertical stresses change abruptly across the core due to the difference between the stiffness (modulus) of asphalt concrete and the transition materials. The maximum vertical and shear stresses in the dam body are 0.8 MPa and 0.06 MPa respectively.

The computed results show that the maximum settlement occurs at the middle height of the dam in the core and transition zones and is of the order of 11cm. The horizontal displacements are symmetrical as would be expected, and the maximum value is 2 cm at the downstream and upstream shells.

#### 4-2 Dynamic Analyses

The three dimensional response analyses were carried out using an elasto-plastic

model (Mohr-Coloumb) for the dam body materials and asphalt core and an elastic model for its rock foundation. These analyses were performed under different earthquake loadings with three levels of seismic risk [20] as follow:

- The Friuli earthquake in Italy (1976) with the magnitude of  $M_b=6$  and  $a_{max}=0.25g$  as a design basis level (DBL).
- The Irpinia earthquake in Italy (1980) with the magnitude of  $M_b=6.8$  and  $a_{max}=0.5g$  as a maximum design level (MDL).
- The Manjil earthquake in Iran (1990) with the magnitude of  $M_b=7.3$  and  $a_{max}=0.6g$  as a maximum credible level (MCL).

As there are two horizontal components for each earthquake acceleration, the more critical component was selected as the bedrock motion.

According to the ICOLD classification [20], Meyjaran dam is not classified as a very high-risk dam since its reservoir is small and there is not any substantial residential and industrial installation in its downstream. Therefore to design this dam, the seismic loads are derived from MDL and DBL earthquakes, and controlling for the earthquake level of MCE is not required. However, in order to investigate the effects of a very severe earthquake, dynamic analyses of this dam under Maximum Credible Earthquake level (MCL) have also been performed and the results are discussed in this paper.

#### 4-3 Results of Dynamic Analyses

The acceleration time history of the Friuli Earthquake ( $a_{max}=0.25g$ ) as input motion is shown in Figure 9. A comparison between the

response acceleration at the dam crest (Figure 10) with the input motion shows that the maximum horizontal acceleration at the dam crest has reached 0.73g giving a magnification factor of 2.9. In spite of this high acceleration at the dam crest, the induced displacements are small. The maximum horizontal displacement at dam crest is equal to 6.3cm. The results also show that the induced shear strain in the asphalt core is less than 1% (Figure 11) .

After scaling to the maximum design level earthquake, Irpinia earthquake ( $a_{max} = 0.5g$ ) was used as an input motion. The obtained results indicate that the maximum horizontal displacement of the dam body was 32.4cm towards the upstream. At this stage, the dam crest horizontal displacement is 18.7 cm (Figure 12). The time history of acceleration at the dam crest is shown in Figure 13. It is observed that the maximum crest acceleration has reached 0.89g with a magnification of 1.8. The shear strains induced in asphalt core are less than 6%.

For earthquake loading with the maximum credible level, the Manjil earthquake was selected as the input motion after scaling to 0.60g (Fig 14). Figure 15 shows the time history of acceleration at the dam crest. It is seen that seismic waves are strongly amplified in the dam body (and its foundation), and the dam crest motion is much stronger than the input motion such that the acceleration at dam crest reaches 1.6g. However, the maximum response acceleration does not occur at the dam crest but at mid height of the dam (Figure 16).

The variation of horizontal acceleration at the crest along the dam is seen in Figure 17. It is observed that the response acceleration is suddenly increased at the deepest point of the valley, and also the maximum acceleration is

induced at rock abutments of the dam.

The shear strain level on the longitudinal section of the core wall is shown in Figure 18. The induced shear strains are relatively small everywhere within the core (less than 4%), except for the upper part of the core where the level of shear strain reaches a maximum of 14% at the dam crest.

According to the test results, at the upper part of the asphalt core of the dam, where the dynamic analyses under a severe earthquake (MCL), gave large shear strains (around 14%), it is expected that the permeability is increased. However, these deformations are only induced in a very limited depth at the top of core. Therefore, any possible shear cracks will not release significant water from the reservoir to the downstream and the design criteria are satisfied.

In spite of relatively small deformations in the asphalt core, there is a large induced deformation and shear strain in the transition material adjacent to the core. Figure 19 shows variation of the shear strains in the core and transition material along the height of dam, at the center section of the dam. The core and transition zone have similar deformations and act together in the range of small strains up to a height of about 35m, but thereafter the transition zone shows very high strains and large deformations. For the lower part of the dam (about 2/3 height) the transition and the core have almost elastic behavior with the same deformation, while at the upper part, the transition material behaves as a plastic material with deformations quite different from those in the core. In the analyses, using plasticity constitutive models such as Mohr-Coulomb, a significant amount of energy dissipation and a high damping ratio (up to 0.63) can occur during plastic flow. While in a real

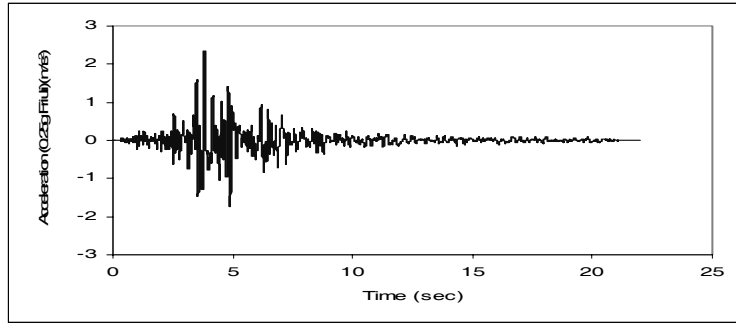


Figure 9: Acceleration. time history of Input Motion (Friuli Earthquake)

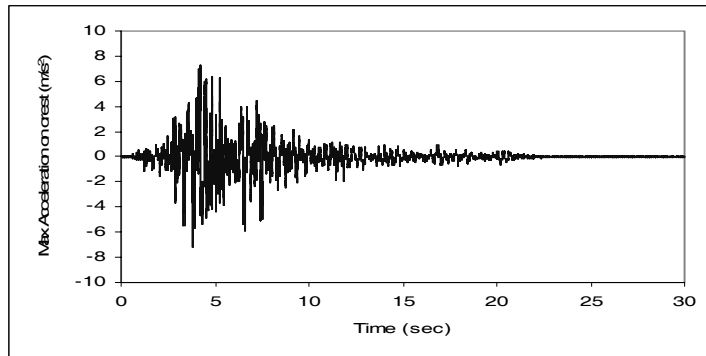


Figure 10: Acceleration response of dam at crest (Friuli Earthquake)

### Contour of Shear Strain Increment

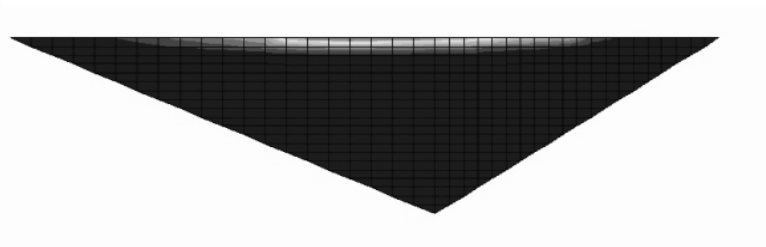
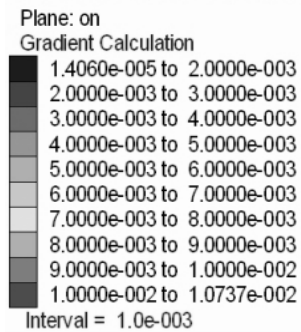


Figure 11: Shear strain levels on the longitudinal section of asphalt core wall (Friuli Earthquake)

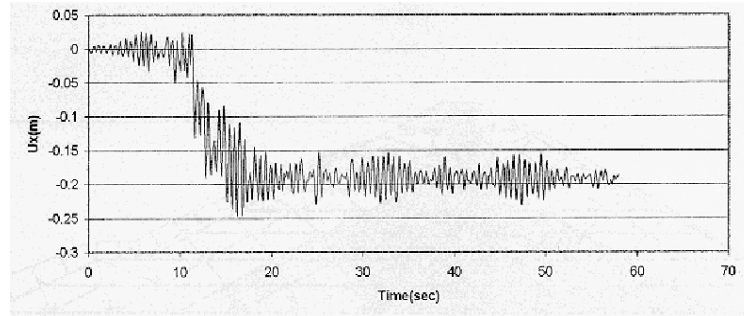


Figure 12: X-displacement response of the dam at crest (Irpinia Earthquake)

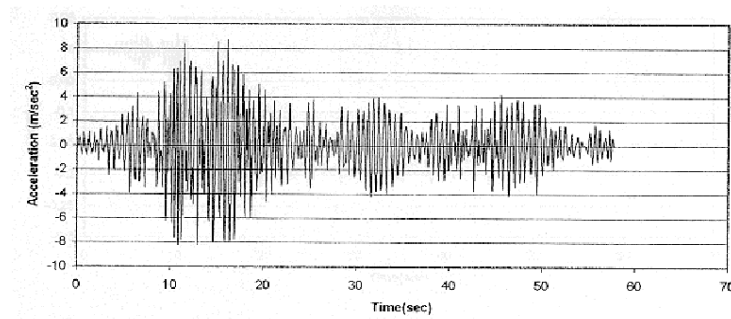


Figure 13: Acceleration response of the dam at crest (Irpinia Earthquake)

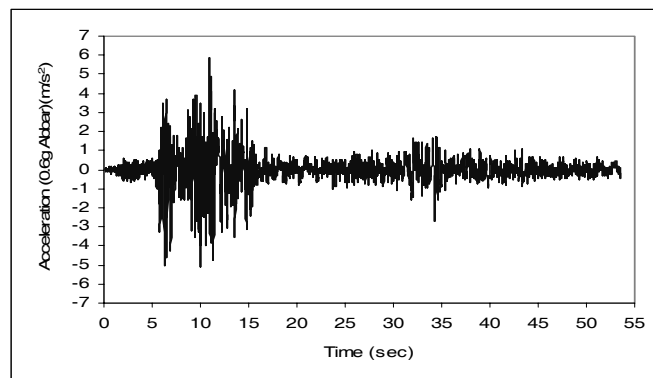


Figure 14: Acceleration. time history of Input Motion (Manjil Earthquake)

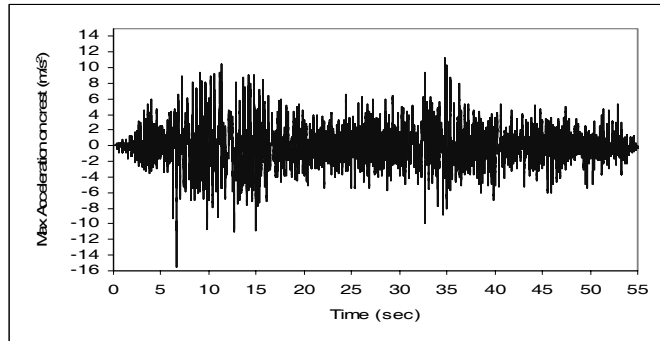


Figure 15: Acceleration response of dam at crest (Manjil Earthquake)

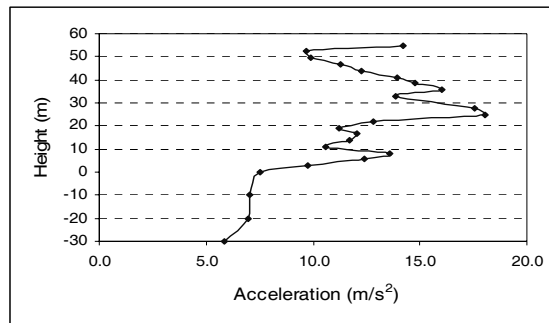


Figure 16: Max. accelerations along the height of the dam (Manjil Earthquake)

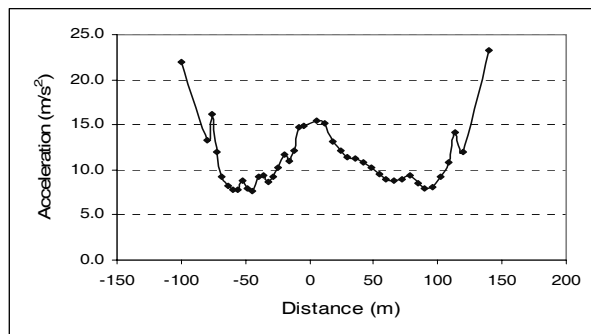


Fig. 17: Variation of horizontal acceleration at dam crest along the longitudinal axis (Manjil Earthquake)



### Contour of Shear Strain Increment

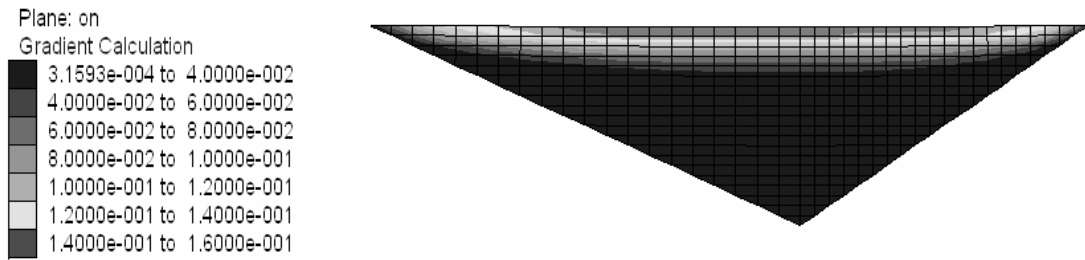


Figure 18: Shear strain levels on the longitudinal section of asphalt core wall(Manjil Earthquake)

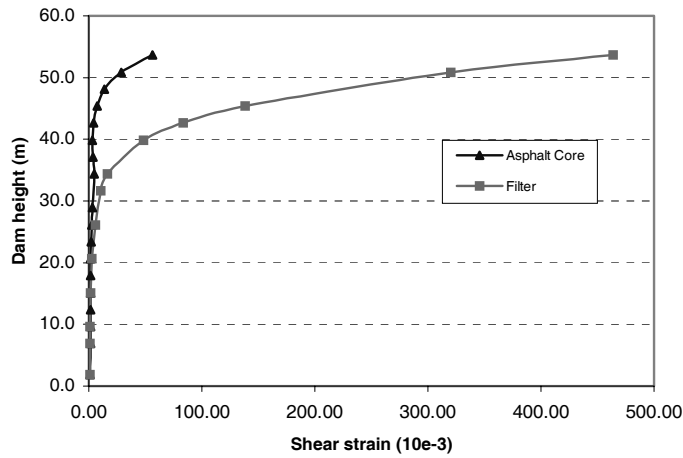


Figure 19: Variation of the shear strains in the core and filter along the height of the dam(Manjil Earthquake)

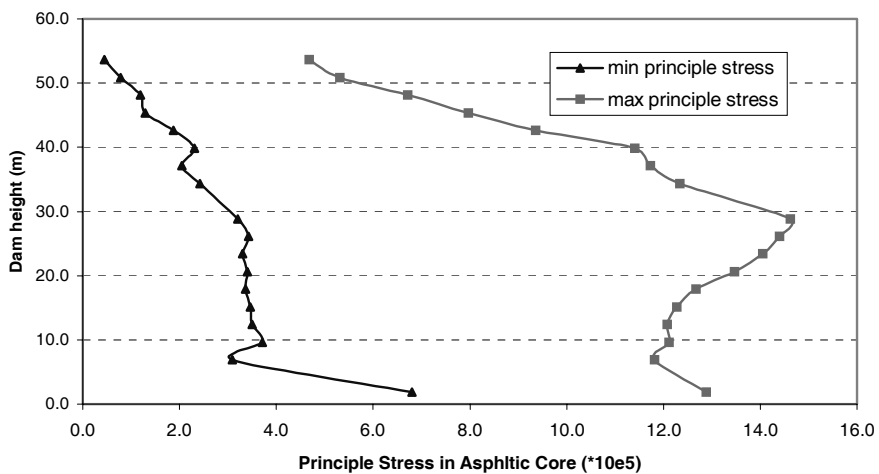


Figure 20: principal stresses in the core along the height of dam (Manjil Earthquake)

Table 7: Permeability test results

Axial strain %	Permeability (cm/s)
3	impermeable
6	impermeable
10	$10^{-6}$
14	$10^{-5}$

case, gravel may not exhibit such high damping even at large strain. Laboratory tests on asphalt concrete showed that the damping ratio may reach 55% at strains of 1% and higher [12].

The analyses of induced stresses in the asphalt core dam shows that the normal stresses in all parts of core are in compression, and no tensile stress is induced in the core even under strong motions (Figure 20 ). Therefore no tensile cracking should be expected. A summary of obtained results for the dam deformations is presented in Table 7.

## 5 Conclusions

In this study, in order to investigate the dynamic behavior of asphalt concrete core dams under earthquake loading, an extensive numerical analysis was carried out. To determine deformation properties for use in the numerical models, laboratory tests including static and cyclic triaxial tests and wave velocity measurements by the pulse method have been performed on asphalt samples. Also, to study the effect of induced shear strain on the permeability of asphalt concrete, permeability tests have been conducted. From the results of this study, the following conclusions have been drawn:

1- The cyclic triaxial tests data show that the dynamic shear modulus,  $G$ , of asphalt material is strongly dependent on the shear strain.

2- The triaxial tests under cyclic shear stress of 0.1 to 0.2 MPa, which corresponds approximately to the load of earthquakes with Richter magnitude 6.0 to 6.8, acting on Meyjaran asphalt core dam, show that the induced deformations on samples of asphalt concrete core material are very small and there is no sign of any material deterioration or cracking.

3- Three-dimensional non-linear dynamic analyses of Meyjaran rockfill dam with asphalt concrete core under different levels of earthquake loadings showed that the input motion is strongly amplified in the dam body and its foundation for all levels of earthquake loadings with a high magnification factor for response accelerations. The maximum acceleration is induced at rock abutments of the dam.

4- Under moderate earthquake loading using the Friuli earthquake with  $a_{max} = 0.24g$ , and also a strong earthquake; Irpinia with  $a_{max} = 0.5g$ , the induced deformations in dam body are small and the shear strains in the asphalt core are less than 1% and 6%, respectively. In these ranges of deformations, according to the results of permeability tests, the asphalt core remains watertight. Therefore, it is expected that no damage will occur to the Meyjaran dam during operation.

5- Under a very severe earthquake; Manjil earthquake with  $a_{max} = 0.6g$  (MCL), the induced shear strains in most parts of the asphalt core zone are small, except for its

upper part. For the case studied in this research, the level of shear strain reaches a maximum value of 14% at the dam crest. According to the laboratory test results, the permeability of the asphalt will increase in this range of core strain. However, considering that the location of these deformations is at the top of the asphalt core, the dam is still safe.

These results have indicated that the asphalt-concrete core behaves safely even under a very severe earthquake and it can satisfy the seismic design criteria under DBL, MDL and MCL levels of earthquake loadings.

The results obtained in this study should be reviewed and re-evaluated when data on seismic behavior of asphalt concrete core dams become available.

### Acknowledgements

The authors would like to thank Professor Hoeg (Norwegian Geotechnical Insitute) for his fruitful discussion about this subject and valuable comments on this research. Sincere thanks are also due to Dr. Ali Noorzad (Iran Water Resources Management Organization, IWRMO) for his assistance and support during this study and Dr. M.K. Jafari (International Institute of Earthquake Engineering and Seismology) for his support to perform the cyclic triaxial tests.

### References

- [1] Hoeg, K., [1998]. "Asphalt Core Embankmen damts", Dam Engineering, Vol IX, Issue 3.
- [2] Creegan, P.J.,and Monismith, C.L., [1996], " Asphalt-Concrete Water Barriers for Embankment Dams", ASCE, New York, USA
- [3] Norwegian Geotechnical Institute, NGI, [2005], Earthquake Resistance of Asphalt Core Embankment Dams Report No. 2005103101, Norway.
- [4] Baziar M.H., Noorzad A, Salemi Sh., Ghannad Z., [2003], "Evaluation of Earthquake response of 15th Khordad Earth Dam", Proceedings of 21st ICOLD International Congress, Canada, Montral.
- [5] Hoeg, K., [1993]. "Asphaltic Concrete Core Dams", Norwegian Geotechnical Insitute, Norway.
- [6] Gurdil, A.F., [1999]. "Seismic Behavior of an Asphaltic Concrete Core Dam", Proc. Of 1st Symposium on Dam Foundations, Antalya, Turkey.
- [7] Ghanooni, S.M. and Roosta, R.M. [2002]. "Seismic Analysis and Design of Asphaltic Concrete Core Embankment Dams," International Journal of Hydropower and Dams, Issue b, pp. 75-78.
- [8] Salemi, Sh. and Baziar, M.H., (2003). "Dynamic Response Analysis of a Rockfill Dam with Asphalt-Concrete Core", Proc. of Soil and Rock American Conference, MIT, Boston.
- [9] Baziar.M.H., Merrifield C.M., Salemi Sh. and Heidari T, [2004], "Three Dimensional Dynamic Analysis of Alborz Dam with Asphalt and Clay Cores", CD Proceedings of Fifth International Conference on Case Histories in Geotechnical Engineering, New York, NY.
- [10] Breth H., Schwab H., [1973], "Stresses on Asphaltic Concrete Cores in High